STATUS OF THE TWO-DIMENSIONAL SYNCHROTRON RADIATION INTERFEROMETER AT PETRA III*

A.I. Novokshonov, A.P. Potylitsyn,Tomsk Polytechnic University (TPU), Tomsk, Russia
G. Kube, M. Pelzer, G. Priebe, Deutsches Elektronen-Synchrotron (DESY), Hamburg, Germany

Abstract

Synchrotron radiation based emittance diagnostics at modern 3^{rd} generation light sources is mainly based on beam profile imaging in the X-ray region in order to overcome the resolution limit imposed by diffraction. A possibility to circumvent this limitation is to probe the spatial coherence with a double-slit interferometer in the optical spectral region. The light source PETRA III at DESY is using this type of interferometer since several years in order to resolve vertical emittances of about 10 pm.rad. The device is set up behind a 30 m long optical beamline, connecting the accelerator tunnel and the optical hutch. In order to increase the measurement stability, a much shorter optical beamline with reduced number of optical elements was recently commissioned. At the end of the beamline, a two-dimensional interferometer was installed which allows to deduce transverse emittances in both planes simultaneously. This contribution summarizes the status of beamline and interferometer commissioning.

PRINCIPLE

The principle of the interferometric method is based on the investigation of the spatial coherence of SR. In order to quantify the coherence properties usually the first order degree of mutual spatial coherence $\gamma(D)$ is used (c.f. for example Ref. [1]) with D the distance between two wavefront dividing slits, see Fig. 1. The interferometer itself is a wave-front–division-type two-beam interferometer which uses polarized quasi monochromatic radiation. The intensity of the interference pattern (interferogram) measured in the detector plane directly depends on γ [2]:

$$I(y_0) = I_0 \left[\mathrm{sinc}(\frac{2\pi a}{\lambda R} y_0)\right]^2 \left[1 + |\gamma| \cos(\frac{2\pi D}{\lambda_0 R} + \varphi)\right] \quad (1)$$

with a the half of the single slit height and D, R as indicated in Fig. 1, λ_0 the wavelength of observation and I_0 the sum of the incoherent intensities from both slits. If the condition of Fraunhofer diffraction (i.e. far–field limit) holds, the van Cittert–Zernicke theorem [3] relates the degree of coherence γ with the normalized source distribution $f(y)$:

$$\gamma(\nu) = \int \mathrm{d}y f(y) \exp(-i2\pi\nu y) \,, \quad (2)$$

where $\nu = \frac{D}{\lambda_0 R_0}$ denotes the spatial frequency. The beam size information is encoded in the interferogram such that as smaller the beam size, as deeper the modulation depth of the interference pattern. In the case of an ideal point source, the intensity in the minima of the pattern would amount to $I_{min} = 0$, resulting in a visibility of $V = \frac{I_{max} - I_{min}}{I_{max} + I_{min}} = |\gamma| = 1$. The visibility of an extended source will always have a visibility $V < 1$.

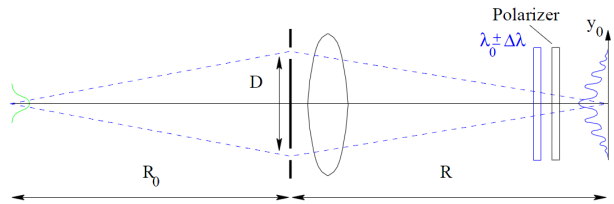

Figure 1: Principle setup for interferometric beam size measurements.

If the beam shape $f(y)$ is known to be normal distributed with width σ_y, the integral in Eq. (2) can be solved analytically which results in an equation by which the beam size can directly be determined:

$$\sigma_y = \frac{\lambda_0 R_0}{\pi D} \sqrt{\frac{1}{2} \ln \frac{1}{\gamma(D)}} \,, \quad (3)$$

while $\gamma(D)$ has to be fitted from the recorded interferogram. A comprehensive overview and more details about the development of SR interferometers can be found in Ref. [4].

EXISTING SETUP

Since 2011 an interferometric measurement is in use at the 3^{rd} generation light source PETRA III at DESY, Hamburg (Germany) in order to resolve the small vertical emittance of $\varepsilon_y = 10$ pm rad. The setup is installed behind an about 30 m long optical beamline which is described in Ref. [5]. However, this setup suffers from many problems:

(i) Due to the long distance between source point and slits the setup is very sensitive on temperature drifts, a correlation between measured emittance values and ambient temperature is visible. (ii) The beamline is equipped with several optical elements (3 lenses and 6 mirrors), each of them introducing additional uncertainties. (iii) The interferometric setup occupies the place of the streak camera, i.e. simultaneous measurements of vertical and longitudinal beam sizes are not possible. (iv) The present interferometric setup allows to measure only vertical beam sizes, a simultaneous horizontal interferometric measurement would be preferable.

In order to overcome these problems, a new optical beamline with extended interferometric setup was installed in

* This work was partly supported by the Russian Federation Ministry of Science and Education within the program "Nauka" Grant # 3.709.2014/K.

ISBN 978-3-95450-177-9

PETRA III and recently put into operation. This new setup and first commissioning results will be presented in the subsequent sections.

NEW INTERFEROMETRIC BEAMLINE

Fig. 2 shows a sketch of the new optical diagnostics beamline together with the interferometer setup. The light extraction point SOL 19 for bending magnet synchrotron radiation (SR) is located about 70 m away from the injection point in the PETRA storage ring. The distance from the SR source point inside the dipole magnet to the extraction mirror is the same than in the old beamline, also the dipole magnet and the extraction chamber are of the same type than in the previous setup and therefore described in Ref. [5].

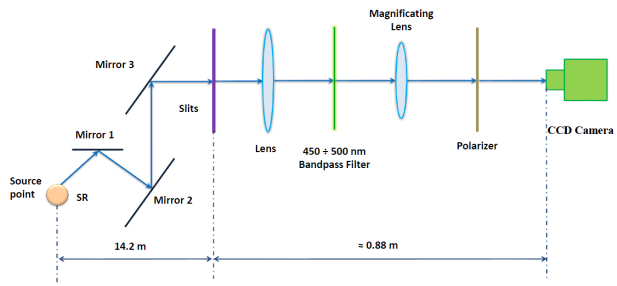

Figure 2: Sketch of the new optical diagnostics beamline together with the interferometer. Mirror 1 is an integrated part of the extraction chamber and deflects the light horizontally to the inner part of the PETRA ring. Mirror 2 and 3 are located in air: mirror 2 deflects the light in vertical direction out of the tunnel to the measuring hut which is sitting on top of the tunnel roof, mirror 3 deflects the light back to the horizontal direction in the direction of the interferometer setup which is mounted onto an optical table.

The light is guided out of the tunnel by mirror 2 and then adjusted to the interferometer by mirror 3. The interferometer consists of the slit system, a lens (Borg 50 ED, f' = 500 mm) with nominal focal length of 510 mm, a bandpass filter (FWHM = 10 nm), a magnification lens to widen the interference pattern, a Glan–Thomson polarizer to select the σ–polarization (Karl Lambrecht Corporation, MGT25S20), and a CCD camera (JAI BM-141GE) to record the interferograms. CCD readout was performed based on the TINE AVINE video system [6, 7].

During the beamline and interferometer commissioning, several bandpass filters in the range from 450 nm to 500 nm were under investigation. Finally it was decided to operate the monitor with a central wavelength of 450 nm because of the better resolution and still sufficient intensity.

As can be seen from Fig. 2, in the new setup the number of mirrors is reduced by a factor of two and no more lenses are required. Moreover, the distance between source point and slits amounts to 14.2 m and therefore is more than two times shorter than in the previous setup. With the reduced number of optical elements and the shorter overall beamline length, the situation should be considerably improved having in mind the list of problems (points (i) and (ii)) from the previous section. In addition, with the new beamline the previous one will be ready to bring back the streak camera into operation, such allowing simultaneous measurements of transverse and longitudinal beam sizes and eliminating point (iii) from the list of problems.

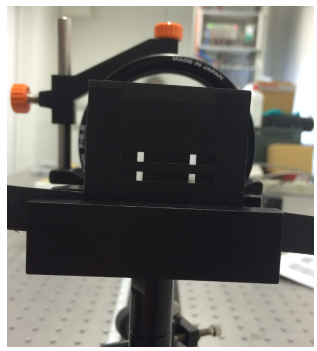

Figure 3: Slit system of the two–dimensional interferometer.

In order to extend the setup for emittance diagnostics in both transverse planes (problem (iv)), it is possible to set up two one–dimensional interferometers by splitting the wave front as it was done in Ref. [8]. However, this would increase the complexity of the setup and introduce an additional optical element in the light path which might distort the wavefront. Therefore it was decided to set up a two–dimensional interferometer as it was done before at SPring–8 in Japan [9].

A photo of the slit system in use is shown in Fig. 3. The horizontal distance between the slits amounts to 7 mm, the vertical one to 16 mm. The slit widths is 1 mm. Mirror 2 rotates the interferogram by 90^o, therefore the slits are rotated by the same angle as can be seen from the photo.

In order to operate and control the interferometer from the accelerator control room a Matlab© client application shown in Fig.4 was developed which allows the communication with the TINE Video server and performs online data analysis. The analysis is performed based on two one–dimensional fits using two data sets for the horizontal and vertical plane which are extracted from a small region around the central part of the recorded interferogram.

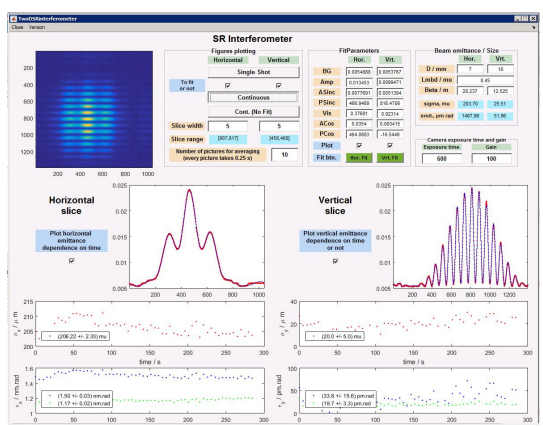

Figure 4: Matlab interface for control and online–analysis.

ISBN 978-3-95450-177-9

OPERATIONAL EXPERIENCE

After the beamline commissioning first beam sizes were obtained. Measured sizes are listed in Tab.1 together with the design values. The error in the horizontal beam size is in the order of 1% and in the vertical one in the order of 10%.

Table 1: Comparison of Beam Sizes

parameter	vertical	horizontal
beam size (measured)	20 μm	180 μm
beam size (design)	12 μm	184 μm

As can be seen the horizontal measurement is in good agreement with the design value, but for the vertical one the difference is about a factor of two. It is assumed that this difference is caused by vibrations which directly can be observed. For illustration Fig.5 shows three consecutive shots, recorded with a small CCD exposure time t_{exp}. As can be seen the position of the interferograms is changing from shot to shot such that an interferogram taken with longer t_{exp} for intensity accumulation would be smeared out, resulting in an increase in the extracted beam sizes. In the horizontal plane this influence is considerably less pronounced because of the larger beam size, but in the vertical plane it clearly affects the measurement.

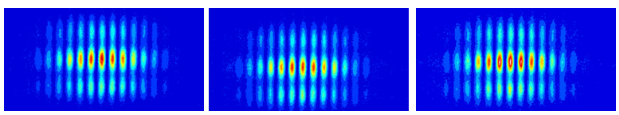

Figure 5: Three consecutive interferograms, recorded with a small CCD exposure time.

In order to support this assumption, vertical emittance measurements were carried out as function of the CCD exposure time which are shown in Fig. 6. It is obvious from this figure that the extracted emittances are considerably smaller for smaller t_{exp}, thus corroborating the vibrational influence. Considering the strong increase in the vertical beam size in the region of $t_{exp} = 300 - 400\ \mu s$, the excitation frequency seems to be in the order of a few kHz.

In order to overcome this limitation a straightforward solution would be to operate the CCD only with small exposure

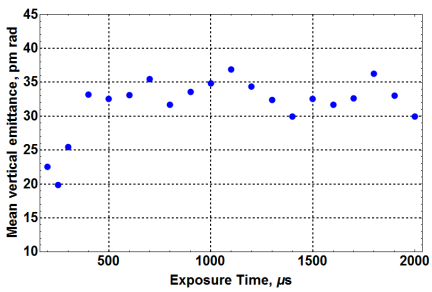

Figure 6: Vertical emittance measurement as function of the CCD exposure time.

times. However, in this case the intensity of the recorded images is rather low and it turned out that the fit for the vertical beam size determination is rather unstable. This effect is illustrated in Fig. 7 where emittance values even higher than 100 pm rad were sometimes generated.

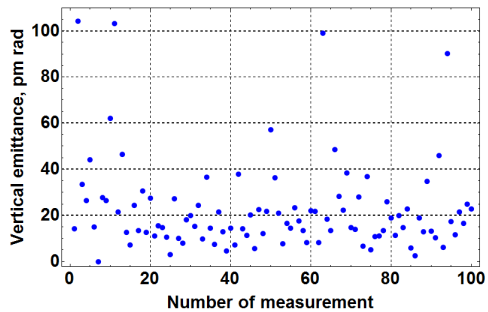

Figure 7: Series of 100 consecutive vertical emittance measurements for $t_{exp} = 200\mu s$.

To avoid the vibrational influence and get comparable results it was decided to use an algorithm which was successfully implemented before at the interferometric beamline of the ALBA light source in Spain [10]. According to this method several interferograms are recorded with small CCD exposure time and finally summed up to have sufficient intensity for a reliable fit operation. However, before summing up each interferogram is shifted in position relative to each other such that the position of the central maximum in all images will be the same.

The result of this technique is shown in Fig. 8 where corrected and uncorrected interferograms are plotted for both planes. From this comparison it is obvious that the correction will improve the beam size determination. In addition, Fig.9 shows two interferograms taken under different conditions: the left one is a superposition of 5 corrected interferograms with 150 μs exposure time, the right one is a single interferogram with 750 μs exposure time. In fact both interferograms have the same total exposure time, but the interference pattern in the corrected on is much sharper compared to the uncorrected.

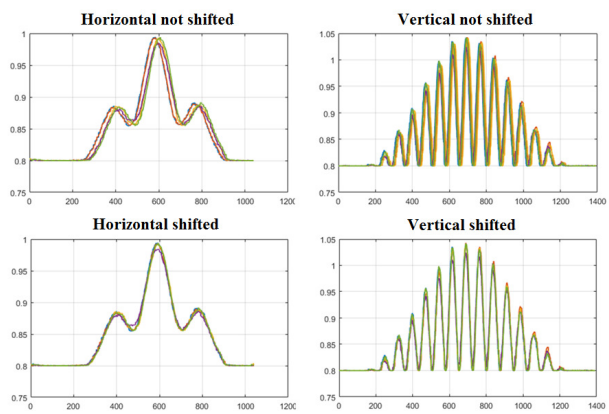

Figure 8: Comparison of position corrected and uncorrected interference patterns for both planes.

ISBN 978-3-95450-177-9

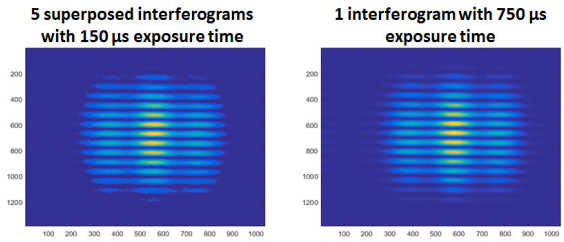

Figure 9: Comparison of corrected and uncorrected interferograms for the same total CCD exposure time.

In Fig.10 100 vertical consecutive emittance measurements are plotted, using the correction algorithm with 20 superposed interferograms at a CCD exposure time of 200 μs. Compared to the results shown in Fig.7 which were taken for the same t_{exp} but based on a single interferogram, it is obvious that the correction stabilizes the fitting algorithm due to the higher statistical significance resulting from the higher intensity. With the help of this correction presently

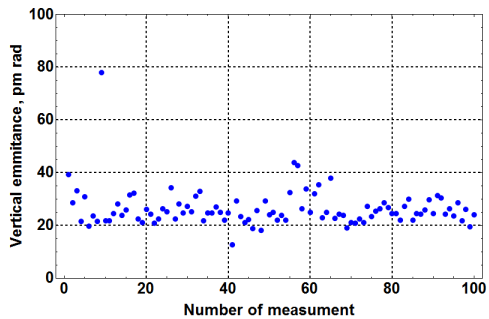

Figure 10: 100 consecutive vertical emittance measurements using the correction algorithm with 20 superposed interferograms at a CCD exposure time of 200 μs.

vertical beam sizes down to 15.5μm can be resolved which are close to the design value of 12μm according to Tab.1.

However, drawback of the correction is the increase in time which is required in order to generate a beam size information: for a single interferogram it takes about 0.25 s to extract beam parameters, if the correction is based on several interferograms this time has to be multiplied by their number in first order.

SUMMARY AND OUTLOOK

In this report the commissioning of a new optical beamline for a two–dimensional interferometric setup at the light source PETRA III is presented together with first operational experiences. It is shown that the new setup avoids the inherent disadvantages of the old one and provides online emittance diagnostics in both transverse planes.

The new setup is limited in the vertical plane by image stability issues caused by vibrations. A correction algorithm is presented by which it is possible to reduce this influence and to extract beam sizes close to the design values.

The origin of these vibrations is still an open question. The beam stability in the vicinity of the radiation source point was investigated based on turn–by–turn measurements with the BPM system, resulting in a (rms) beam stability of about 1 μm in the vertical plane and 1.7 μm in the horizontal one, thus being to small to explain the observations. Presently different causes are under investigation.

Apart from this problem the new setup is already in use for online emittance diagnostics in the accelerator control room, both for daily emittance control and for dedicated machine studies. As an example, Fig.11 shows a screen shot of the monitor panel where a sudden emittance increase caused by ion instabilities is observed.

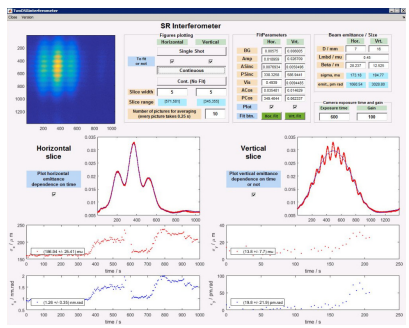

Figure 11: Monitor screen shot showing emittance increase due to ion instabilities.

ACKNOWLEDGEMENTS

The authors thank A. Affeldt, A. Delfs, S. Warratz and R. Zahn (DESY) for substantial help and support during the design and installation of the new beamline.

REFERENCES

[1] M. Born and E. Wolf, Principles of Optics, Pergamon Press Ltd., New York, 1980.

[2] T. Mitsuhashi, Proc. of the Joint US–CERN–Japan–Russia School on Particle Accelerators, Montreux, 11-20 May 1998, (World Scientific), pp. 399-427.

[3] P.H. Van Cittert, Physica **1**, 201 (1934).
F. Zernike, Physica **5**, 785 (1938).

[4] T. Mitsuhashi, Proc. BIW'04, Knoxville (Tennessee), USA, May 2014, AIP Conf. Proc. **319**, 3 (2004).

[5] H.C. Schröder *et al.*, Proc. DIPAC'11, Hamburg, Germany, May 2011, MOPD30, p.113 (2011).

[6] S. Weisse *et al.*, Proc. ICALEPCS'09, Kobe, Japan, October 2009, MOD003, p.34 (2009).

[7] S. Weisse *et al.*, Proc. ICALEPCS'11, Grenoble, France, October 2011, MOPMS033, p.405 (2011).

[8] H.Hanyo *et al.*, Proc. of PAC'99, New York, USA, March 1999, p.2143 (1999).

[9] M. Masaki and S. Takano, Proc. DIPAC'01, Grenoble, France, May 2001, PS17, p.142 (2001).
M. Masaki and S. Takano, J. Synchrotron Rad. **10** (2003), 295.

[10] L. Torino and U. Iriso, Proc. IBIC'15, Melbourne, Australia, September 2015, TUPB049, p.428 (2015).

ISBN 978-3-95450-177-9